
Article:
Sala, E.M. orcid.org/0000-0001-8116-8830, Na, Y.I., Godsland, M. et al. (2 more authors) (2020) InAs/InP quantum dots in etched pits by droplet epitaxy in metalorganic vapor phase epitaxy. physica status solidi (RRL) – Rapid Research Letters, 14 (8). 2000173. ISSN 1862-6254

https://doi.org/10.1002/pssr.202000173

InAs/InP Quantum Dots in etched pits by droplet epitaxy in MOVPE

Elisa M. Sala[1,2], Young In Na[2], Max Godsland[2], Aristotelis Trapalis[1,2], and Jon Heffernan[1,2]*
[1]EPSRC National Epitaxy Facility, The University of Sheffield, North Campus, Broad Lane, S3 7HQ Sheffield, United Kingdom
[2] Department of Electronic and electrical engineering, The University of Sheffield North Campus, Broad Lane, S3 7HQ Sheffield, United Kingdom

Dr. Elisa Maddalena Sala
EPSRC National Epitaxy Facility and Department of Electronic and electrical engineering, The University of Sheffield North Campus, Broad Lane,
S37HQ Sheffield,
United Kingdom
E-mail: e.m.sala@sheffield.ac.uk

Young In Na, Max Godsland
Department of Electronic and electrical engineering, The University of Sheffield North Campus, Broad Lane,
S37HQ Sheffield,
United Kingdom

Dr. Aristotelis Trapalis and Prof. Jon Heffernan
EPSRC National Epitaxy Facility and Department of Electronic and electrical engineering, The University of Sheffield North Campus, Broad Lane,
S37HQ Sheffield,
United Kingdom

Keywords: III-V quantum dots, MOVPE, droplet epitaxy, AFM, photoluminescence

Abstract

The growth of InAs Quantum Dots (QDs) on InP(100) via droplet epitaxy in a Metal Organic Vapour Phase Epitaxy (MOVPE) reactor is studied. Formation of Indium droplets is investigated with varying substrate temperature, and spontaneous formation of nanoholes is observed for the first time under MOVPE conditions. Indium droplets are crystallized into QDs under Arsenic flow at different temperatures. For temperatures greater than 500ºC, a local etching takes place in the QD vicinity, showing an unexpected morphology which is found to be strongly dependent on the

crystallization conditions. Such QDs are structurally and optically investigated and emission from single QDs in the telecom C-band is detected via micro-photoluminescence at low temperature.

In the last decades, self-assembled quantum dots (QDs) have attracted great attention due to their large impact on the performances of semiconductor lasers,[1,2] nanomemories[3-6] and quantum information technologies.[7-9] In particular, III-V QDs are efficient sources of pure single photons[7] and entangled photon pairs,[10] and can be easily integrated into photonic chips, thus representing the building blocks for future quantum networks.[7,10] A successful and robust fabrication method for high-quality III-V QDs is the Stranski-Krastanov (SK) growth mode,[11] largely exploited in both Molecular Beam Epitaxy (MBE) and Metal Organic Vapour Phase Epitaxy (MOVPE) environments.[12-14] An alternative technique is Droplet Epitaxy (DE), initially developed by N. Koguchi *et al.*[15] in MBE, which relies on the spontaneous formation of group III metallic droplets which are subsequently crystallized into QDs by the supply of a group V source. Droplet epitaxy is a flexible technique for fabricating high-quality nanostructures, since it does not rely on the lattice-mismatch between substrate and epilayer, and its successful applications can be found for example in single-photon[16] and entangled pairs[17] emitters, and solar cells[18].

One opportunity enabled by DE at high temperatures is the observation of metal induced surface etching to create nucleation sites for further localization of QDs. This so-called local droplet etching (LDE) was first reported by Z. Wang *et al.* .[19] under MBE conditions. LDE is an appealing technique, since QDs positioned in the etched pits generally reveal narrow emission linewidths and small fine-structure-splitting (FSS)[20-22] due to increased spatial symmetry. This has fundamental advantages for achieving a higher degree of entanglement, by reducing the fine-structure splitting of the excitons responsible for entangled photon pair emission.[20] On the other hand, much less attention has been devoted to DE in MOVPE,[23-29] where to date fabrication of QDs via SK still

dominates. Nevertheless, recent development of DE in MOVPE produced high-quality InAs/InP QDs which have shown a smaller FSS compared to SK QDs[26] and led to demonstration of the first Quantum Light-Emitting Diode (QLED) operating around 1.55 μm at temperatures up to 93K.[28] Among III-V QDs systems, InAs/InP QDs are indeed very attractive for fibre-based quantum network applications, due to their compatibility with the low loss telecom C-band.

In this letter, we present a multi-step growth procedure for fabricating self-assembled InAs/InP QDs via DE in an MOVPE environment, leading to the formation of QDs in etched pits. The combination of droplet epitaxy and droplet etching is potentially advantageous since, unlike in previous MBE works, the infilling of etched pits in a separate step is not required. In fact, the droplet crystallization into QDs and the local etching take place at the same time. By adjusting the crystallization temperature, the etch depth around the QDs can be tuned and, at the same time, the QD morphology is considerably affected. We first consider the Indium droplet formation on a bare InP surface and provide details on the growth sequence employed for droplet crystallization into InAs QDs. By using a combination of Atomic Force Microscopy (AFM), Room Temperature Photoluminescence (RT-PL), and Low Temperature Micro-Photoluminescence (LT-μPL), we investigate their morphological and optical properties.

The samples studied in this work were grown in a 3x2 close-coupled showerhead (CCS) Aixtron MOVPE reactor, using H_2 as carrier gas. The precursors employed are trymethylindium (TMIn) for the Indium droplets, phosphine (PH_3), and arsine (AsH_3), for InP growth and droplet crystallization into QDs respectively. For droplet formation, Indium was supplied at a constant TMIn flow of 2.6 μmol/min for 35 s after the growth of ~300 nm InP buffer layer. **Figure 1** shows AFM micrographs of Indium droplets deposited on the bare InP (100) buffer surface, at substrate temperatures ranging from 300°C to 400°C. Indium droplets form and, as a result of metallic diffusion, the droplet density decreases with temperature from $3x10^9$ cm^{-2} to $6x10^7$ cm^{-2} for 320°C

and 400°C respectively. Droplet dimensions vary accordingly, increasing proportionally with temperature from ~ (35 ± 7) nm width and ~ (6 ± 2) nm height to ~ (200 ± 20) nm width and ~ (32 ± 5) nm height for 320°C and 400°C, respectively. One limitation of DE in MOVPE is that the growth temperature and Indium deposition are not independent, as they are in MBE,[30] and we observe that below 300°C (**Figure 1(a)**) no droplets can be detected when the TMIn used as Indium precursor material is not pyrolyzed. In **Figure 1D** a 3D micrograph shows a more detailed view of nanoholes that are formed on the InP surface, where Indium droplets and nanoholes co-exist. The typical nanohole depth is ~ (1 ± 0.5) nm and ~ (30 ± 5) nm wide, with density of ~10^9 cm^{-2}. On closer inspection, the profiles of such holes strongly resemble the nanoholes spontaneously formed during DE in MBE, as reported for example in Z. Wang *et al.* .[19] To our knowledge, this is the first observation of such spontaneous nanoholes formation in MOVPE, when no group V flow is provided to the group III metallic droplets. Further experimental investigations are needed to confirm the exact physical mechanism behind the formation of such nanoholes. Next, in order to study QD formation, Indium droplets were exposed to an AsH_3 flow.

The full growth sequence is as follows: **(i)** growth of an InP buffer layer at 600ºC, **(ii)** cooling down to droplet deposition temperature under PH_3 for surface stabilization, **(iii)** Indium deposition without any group V precursor for droplet formation, **(iv)** heat up under an AsH_3 flow of 24 µmol/min, (**v)** stabilization under AsH_3 for complete droplet crystallization, (**vi)** InP capping layer at the same temperature, and (**vii)** final InP layer to bury the QDs for PL emission. For AFM investigations, the growth procedure is terminated after the stabilization step **(v)**, and the samples are immediately cooled down to room temperature. **Figure 2** shows AFM micrographs of free-standing InAs QDs on bare InP surfaces, originating from crystallisation of droplets deposited at 320ºC (as in **Figure 1B**).

Here, the droplet crystallization temperature has been varied in the range 480ºC – 530ºC, and three

main features can be distinguished with increasing temperature: **(i)** increase of QD density, **(ii)** increase in the magnitude of the locally etched region around each QD, **(iii)** alteration of QD size. In the temperature range used, the QD density varied from $4 \cdot 10^8$ to a maximum of $9 \cdot 10^8$ cm^{-2} at 520ºC, without supplying any additional material in terms of TMIn or AsH_3 flows. QD dimensions increase with temperature up to 520ºC, while a clear size reduction is observed at 530ºC, see **Figure 2D**. From analysis of a large number of dots, typical QD dimensions at 480ºC are ~ (5±2) nm and ~ (45±7) nm, for height and width respectively. At 520ºC and 530ºC, QDs show a bimodal size distribution. At 520ºC they have diameters of ~ (56±7) nm and ~ (45±5) nm and heights of ~ (15±3) nm and ~ (7±2) nm, respectively; while at 530ºC diameters of ~ (60±5) nm and ~ (35±5) nm and heights of ~ (5±1.5) nm and ~ (2±0.5) nm, respectively are found. This means that from 520ºC to 530ºC the QD aspect ratio has strongly reduced (~ -65%) for both QD populations. More detailed analysis is given in **Figure 3** which shows 3D AFM micrographs of single (double) QDs and illustrates the formation of QDs *within* locally etched pits. These pits start to form at crystallization temperatures above 500ºC as also shown in **Figure 2B-D**. The pit depth increases from 1 nm at 500ºC to 1.8, 2.7, and 3.4 nm at 510ºC, 520ºC and 530ºC, respectively. Interestingly, such profiles appear step-like, suggesting that the etching proceeds layer-wise, and the depth is a function of the crystallization temperature. The same holds true for the width and length which both increase with increasing temperature. In all cases, the etching areas are elongated, most likely due to the intrinsic stress asymmetry along the two crystallographic directions [0-1-1] and [0-11] at the InAs/InP interface[30] (note that the Indium droplets themselves are not elongated, see **Figure 1**).

During the heating up and Arsenic supply steps **(iv)** and **(v)**, no Phosphorous for surface stabilization is provided, and the InP surface is In-rich due to the metallic Indium previously deposited. Hence, it is very likely that at temperatures as high as 500 ºC, it becomes unstable and thus InP can easily dissolve into Indium and Phosphorous atoms, particularly underneath and close

to the Indium droplets, similarly to what is observed for DE in MBE conditions.[19] The more the temperature rises, i.e. from 500 ºC to 520ºC, the more InP dissolves and the more Indium atoms contribute to increasing the droplets' size, resulting in bigger QDs. The dissolved P atoms instead would likely escape into the growth chamber. Note that the In–P bond strength is smaller than In-As, i.e. ~47.3 kcal/mol vs. ~48.0 kcal/mol,[31,32] thus favoring the formation of InAs as part of the QDs over InP, once the In-P bonds are broken. Further increasing the temperature from 520ºC to 530ºC leads to a higher probability for Indium atoms to have enough energy to escape from the droplets, thus not contributing to the formation of the final QDs, hence the crystallized QDs will appear smaller. It has been previously observed that for InAs QDs grown on InP via DE in MOVPE, a non-stoichiometric 2D layer is formed during the Indium droplet exposure to the Arsenic flow during the temperature ramp,[26] here denoted as step **(iv)** of the growth sequence. Such a layer is expected to be formed due to As-P exchange reactions while exposing the In-rich InP surface to Arsenic.[33] It is referred to as a "2D quasi-wetting layer" (WL) and is likely made of $InAs_xP_{1-x}$.[26] This differs from the common WL found in SK QDs, where strain accumulates and is subsequently released via formation of 3D islands.[11,12] From **Figure 3**, it is plausible that the step-like etching is due to parts of such $InAs_xP_{1-x}$ layer in proximity to the QDs being etched away. Evidence for this is seen in **Figure 4** where we present room temperature macro PL spectra from the samples. Samples were excited with a 645 nm diode laser at 75 Wcm^{-2} power density. Various emission lines can be detected, which are labelled **A**, **B**, **C**, and **D**. Peak **A** is found in all samples at the same spectral position and is ascribed to the InP substrate (ca. 920 nm at RT[34]), and the broad emission band **D** is ascribed to QD emission. It is important to point out that, due to the specific physical properties of the InAs/InP system (lower lattice mismatch compared to the widely studied InAs/GaAs, i.e. ~3% vs. ~7%) the resulting QDs are bigger in size compared to InAs QDs on GaAs. Hence, we expect QDs grown at these conditions to emit at longer wavelength than 1.5 μm at room

temperature, as already observed elsewhere.[35] Moreover, the additional contribution in the range 1900 – 2300 nm seen at T ≥ 500ºC confirms the QD size increase observed in our AFM investigations. Peaks **B** and **C** we attribute to emission from the 2D quasi-WL emission. Interestingly, both these peaks blueshift with increasing droplet crystallization temperature and are eventually completely quenched at 520ºC. In particular, peak **B** emits at 1074 nm for the sample grown at 480ºC, then blueshifts to 1041 nm and finally to 1008 nm for 500ºC and 510ºC, respectively. At greater temperatures, its emission cannot be distinguished anymore from the background. Peak **C** shifts in a similar manner whilst at the same time, the QD emission **D** gains intensity (ca. 50% more for 520ºC compared to 480ºC), suggesting a more efficient carrier recombination into the QDs. We hypothesize that the blueshift and the quenching of peaks **B** and **C** correspond to the increased magnitude of the etching around the QDs as observed in the AFM investigations. From the AFM analysis, we can estimate the total etched area per 1 μm^2: it amounts to ~0.1 μm^2, ~0.3 μm^2 and 0.6 μm^2 for 510ºC, 520ºC and 530ºC, respectively. Hence with increasing temperature, the stepped etching process seen in **Figure 3** leads to a gradual reduction of the average thickness of the 2D layer (the blue shift), and the overall contribution of this layer to the PL decreases as the etch pit size increases and the total area of the 2D layer decreases. Finally, it is important to note that such emission is still detectable at low temperatures (not shown here), which indicates that a contribution to the emission from the 2D layer is still present, but overall much weaker due to the etching.

Finally, in the inset of **Figure 4**, we present low temperature micro-PL from the QDs crystallized at 520ºC. The measurement has been carried out by using a 635 nm laser, and a power density of 4.5 W/cm^2 at 4 K. Emission from single QDs can be clearly detected which confirms the attribution of peak **D** to QD emission. It is worth pointing out that single dot emission is not observed for QDs crystallized at temperatures below 520°C nor at 530ºC. Micro-PL for these samples instead

shows a broad emission but no sharp lines characteristic of single dot emission. In both cases we believe this is due to the presence of significant charge noise which leads to a severe broadening and coalescence of emission peaks.[36] In the case of the lower temperature samples, this is likely due to the effect of the quasi-2D wetting layer which, as can be seen from macro-PL, is still an efficient layer for carrier capture. For the 530ºC sample, it may be due the presence of point defects associated with the AsH_3-stabilized InP surface, as reported by Masut *et al.* [37] Therefore, we believe that 520°C constitutes the optimum temperature for droplet crystallization into high-quality InAs QDs, which can be therefore clearly measured by μPL. Spectra from the sample show a broad range of linewidths up to 125 μeV but a significant proportion of QDs have linewidths less than the 45μeV resolution of the spectrometer. The observation of narrow linewidth single QD emission indicates the high quality of these DE crystallized QDs in MOVPE and with further growth optimization we expect the QDs to be suitable for quantum optics applications, especially in controlling the exciton fine-structure splitting, crucial for photon entanglement.[20]

In conclusion, we have studied the formation of InAs QDs on bare InP (100) surfaces by droplet epitaxy in MOVPE. By varying the droplet crystallization temperature, the QD structural properties are considerably altered. In particular, QDs grown at temperatures greater than 500ºC are positioned in locally etched pits, whose size is directly proportional to the crystallization temperature. Structural and optical investigations show a clear correlation between the etching magnitude and the emission intensities of the 2D-layer and the QD band at room temperature, suggesting that the local etching leads to a more efficient carrier capture into QDs, especially for crystallization temperatures of 520ºC and 530ºC. Additionally, micro-PL investigations showed emission of single QDs around 1.55 μm, with a proportion of dots exhibiting linewidths less than the 45μeV resolution of our spectrometer, thus confirming good optical quality in the telecom C-band and-opening the path for their use in quantum optics applications. We believe that controlling

a growth process that combines droplet epitaxy and droplet etching could lead to improvement of the QD optical properties, and in particular to a reduction of the QD FSS, a key parameter governing the degree of entanglement in single photon pairs.[20] This study represents therefore an important step in the MOVPE growth of high-quality InAs QDs in etched pits emitting at telecom wavelengths. Moreover, the etching process studied here may also be used as a 'defect removal' procedure for DE QDs positioned in pre-patterned hole templates, since most patterning techniques inadvertently introduce defects and impurities.[38]

Acknowledgements

The authors wish to thank Dr Joanna Skiba-Szymanska (Toshiba Research Europe Limited, Cambridge, UK) for fruitful discussions and advice. This work was supported by EPSRC, Grant No. EP/R03480X/1 and by the InnovateUK project Aquasec. The data supporting the findings of this study are openly available in the University of Sheffield data repository at https://doi.org/10.15131/shef.data.12063936.

Received: (( ))
Revised: (( ))
Published online: (( ))

References

[1] N. N. Ledentsov, Semicond. *Sci. Technol.* **2011**, *26*, 014001;

[2] D. Bimberg, U. W. Pohl, *Materials Today* **2011**, *14*, 388;

[3] D. Bimberg, M. Geller, A. Marent, and T. Nowozin, *Memory,* U.S. *8331142 B2,* **2012**;

[4] A. Marent, T. Nowozin, J. Gelze, F. Luckert, and D. Bimberg, *Appl. Phys. Lett.* **2009**, *95*,

242114;

[5] L. Bonato, E. M. Sala, G. Stracke, T. Nowozin, A. Strittmatter, M. N. Ajour, K. Daqrouq, and D. Bimberg, *Appl. Phys. Lett.* **2015**, *106*, 042102;

[6] E. M. Sala, I. F. Arikan, L. Bonato, F. Bertram, P. Veit, J. Christen, A. Strittmatter, and D. Bimberg, *Phys. Status Solidi B* **2018**, *255*, 1800182;

[7] P. Michler, *Quantum dots for quantum information technologies,* Springer **2017**;

[8] D. Castelvecchi, *Nature* **2017**, *541*, 9;

[9] A. J. Shields, *Nature Photonics* **2007**, *1*, 215;

[10] N. Akopian, N. H. Lindner, E. Poem, Y. Berlatzky, J. Avron, D. Gershoni, B. D. Gerardot, and P. M. Petroff, *Phys. Rev. Lett.* **2006**, *96*, 130501;

[11] V. A. Shchukin, N. N. Ledentsov, D. Bimberg, *Epitaxy of Nanostructures*, Springer **2003**;

[12] D. Bimberg, M. Grundmann, N.N. Ledentsov, *Quantum Dot Heterostructures,* Wiley Chichester **1999**;

[13] P. M. Petroff and S. P. Den Baars, *Superlattices and Microstructures* **1994**, *15*, 1;

[14] T. Fukui, S. Ando, Y. Tokura, and T. Toriyama, *Appl. Phys. Lett.* **1991**, *58*, 2018;

[15] N. Koguchi, S. Takahashi and T. Chikyow, *Journal of Crystal Growth* **1991**, *111*, 688;

[16] E. Stock, T. Warming, I. Ostapenko, S. Rodt, A. Schliwa, J. Amaru Töfflinger, A. Lochmann, A. I. Toropov, S. A. Moshchenko, D. V. Dmitriev, V. A. Haisler, and D. Bimberg, *Appl. Phys. Lett.* **2010**, *96*, 093112;

[17] N. Ha*,* T. Mano*,* T. Kuroda*,* Y. Sakuma*, and* K. Sakoda, *Appl. Phys. Lett.* **2019**, *115*, 083106;

[18] P. Yu, J. Wu, L. Gao, H. Liu, Z.Wang, *Solar Energy Materials and Solar Cells* **2017**, *161*, 377;

[19] Z. M. Wang, B. L. Liang, K. A. Sablon, and G. J. Salamo, *Appl Phys. Lett.* **2007**, *90*, 113120;

[20] M. Gurioli, Z. Wang, A. Rastelli, T. Kuroda, and S. Sanguinetti, *Nature Materials* **2019**, *18*, 799;

[21] Y. H. Huo, A. Rastelli, and O. G. Schmidt, *Appl. Phys. Lett.* **2013**, *102*, 152105;

[22] C. Heyn, A. Stemmann, T. Köppen, Ch. Strelow, T. Kipp, M. Grave, S. Mendach, and W. Hansen, *Appl. Phys. Lett.* **2009**, *94*, 183113;

[23] Y. Nonogaki, T. Iguchi, S. Fuchi, Y. Fujiwara, Y. Takeda, *Materials Science and Engineering* **1998**, *B51*, 118;

[24] J. Sormunen, J. Riikonen, M. Mattila, J. Tiilikainen, M. Sopanen, and H. Lipsanen, *Nano Letter* **2005,** *5*, 1541;

[25] T. Ujihara, Y. Yoshida, W. S. Lee, and Y. Takeda, *Appl. Phys. Lett.* **2006**, *89*, 083110;

[26] J. Skiba-Szymanska, R. M. Stevenson, C. Varnava, M. Felle, J. Huwer, T. Müller, A. J. Bennett, J. P. Lee, I. Farrer, A. B. Krysa, P. Spencer, L. E. Goff, D. A. Ritchie, J. Heffernan, and A. J. Shields, *Phys Rev. Appl.* **2017**, *8*, 014013;

[27] A. Shikin, E. Lebedkina, C. Ciostek, P. Holewa, S. Ndoni, K. Almdal, K. Yvind, M. Syperek, and E. Semenova, *Opt. Mater. Express* **2019**, *9*, 1738;

[28] T. Müller, J. Skiba-Szymanska, A.B. Krysa, J. Huwer, M. Felle, M. Anderson, R.M. Stevenson, J. Heffernan, D.A. Ritchie, and A. J. Shields, *Nature communications* **2018**, *9*, 862;

[29] H. Liu, Y. Jin, C. Yang, *CrystEngComm*, **2016**, *18*, 4499;

[30] D. Fuster, K. Abderrafi, B. Alén, Y. González, L. Wewior, L. González, *J. Cryst. Growth* **2016**, *434*, 81;

[31] S. Anantathanasarn, R. Nötzel, P. J. van Veldhoven, T. J. Eijkemans, and J. H. Wolter, *J. Appl. Phys.* **2005**, *98*, 013503;

[32] Y. R. Luo, *Comprehensive Handbook of Chemical Bond Energies,* CRC Press, Boca Raton FL **2007**;

[33] N. Kobayashi and Y. Kobayashi, *Journal of Crystal Growth* **1992**, *124*, 525;

[34] M. Bugajski and W. Lewandowski, *J. Appl. Phys.* **1985**, *57*, 521;

[35] S. Hasan, H Han, M. Korytov, M. Pantouvaki, J. Vanampenhout, C. Merckling, W. Vandervorst, *Journal of Crystal Growth* **2020**, *531*, 125342;

[36] J. Houel, A.V. Kuhlmann, L. Greuter, F. Xue, M. Poggio, B. D. Gerardot, P. A. Dalgarno, A. Badolato, P. M. Petroff, A. Ludwig, D. Reuter, A. D. Wieck, and R. J. Warburton, *Phys. Rev. Lett.* **2012**, *108*, 107401;

[37] R. A. Masut, M. A. Sacilotti, A. P. Roth, and D. F. William, *Can. J. Phys.* **1987**, *65*, 1047;

[38] H. Lan and Y. Ding, *Nano Today* **2012**, *7*, 94.

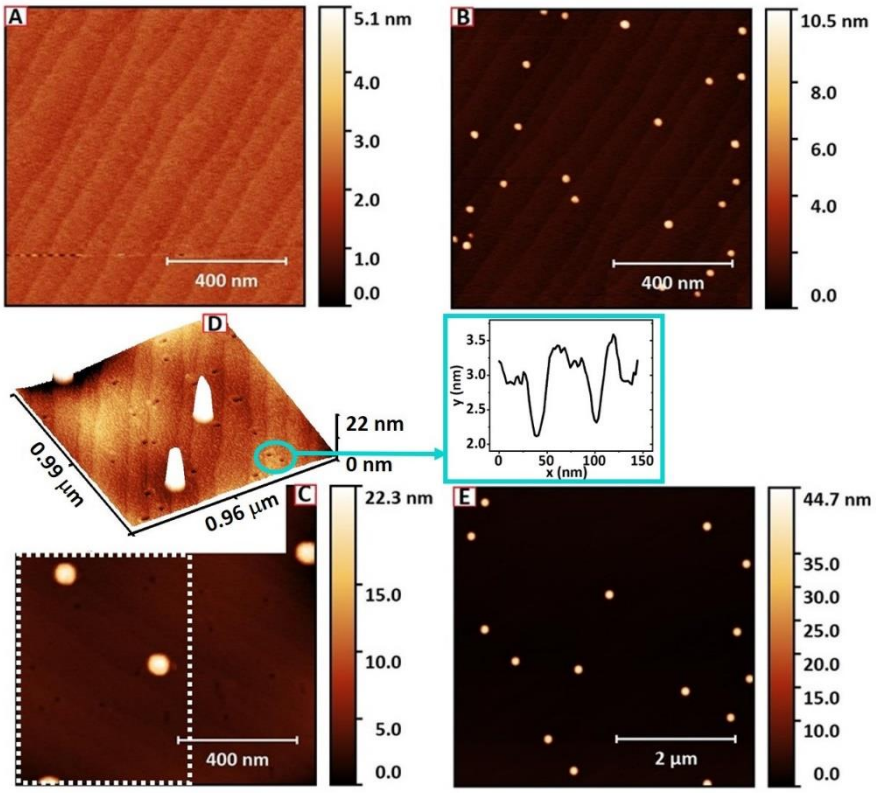

Figure 1. AFM micrographs of Indium droplets deposited on bare InP with increasing temperatures: **A)** 300ºC, **B)** 320ºC, **C)** 350ºC, **E)** 400ºC. In **D)** a 3D micrograph of the dashed area in **C)** is presented. Nanoholes are clearly visible: two of them are highlighted with a blue circle, and their profiles are also shown

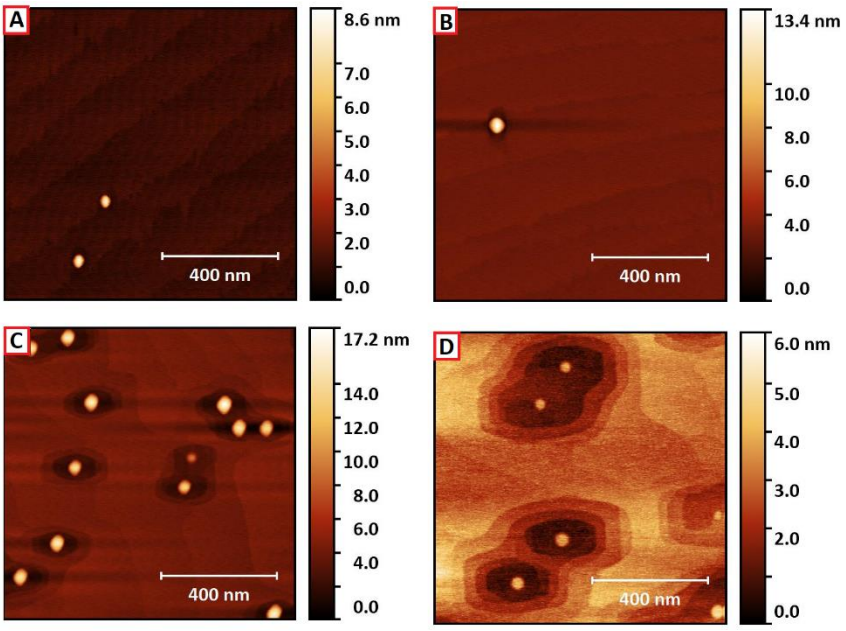

Figure 2. AFM micrographs of free-standing InAs/InP QDs crystallized at different temperature: **(A)** 480ºC, **(B)** 500ºC, **(C)** 520ºC and **(D)** 530ºC.

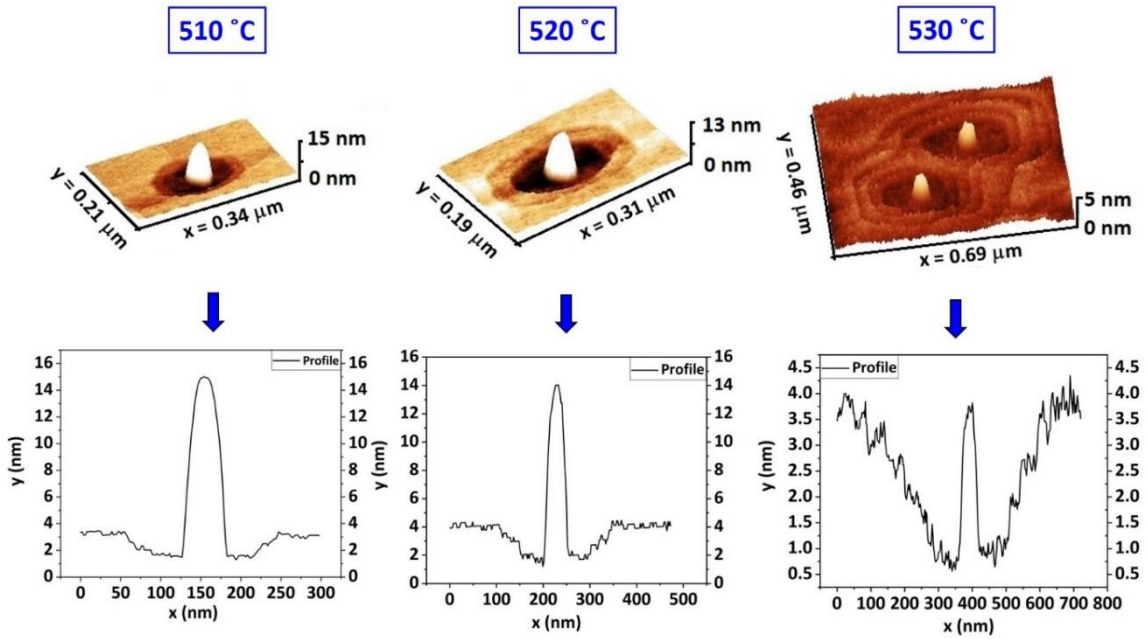

Figure 3. 3D AFM micrographs of QDs and related profiles as a function of crystallization temperature. The lateral dimensions of the etch pits for the considered temperatures are the followings: T=510ºC: (150 ± 10) nm and (100 ± 10) nm. T=520ºC: (240 ± 20) nm and (130 ± 20) nm. T=530ºC: (450 ± 50) nm and (230 ± 20) nm.

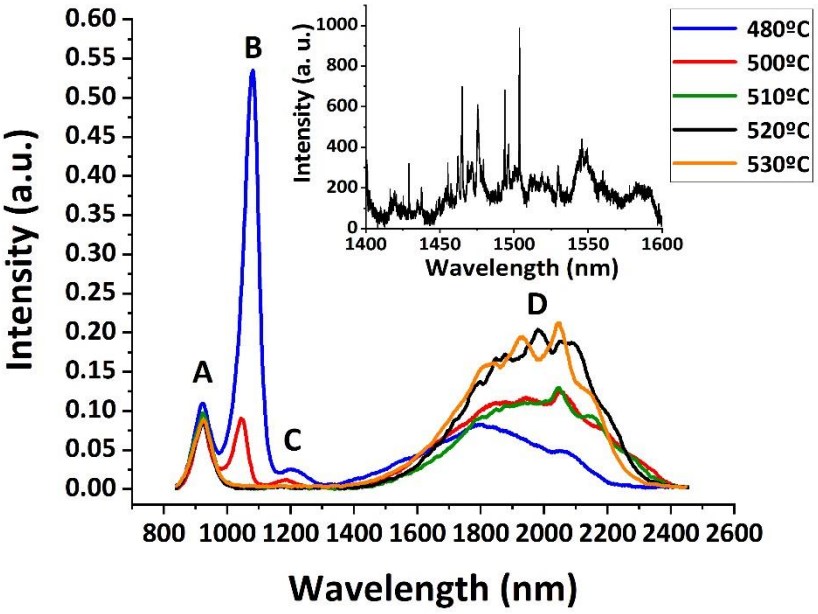

Figure 4. RT-PL of QD samples crystallized at temperatures ranging from 480ºC to 530ºC. The inset displays μPL measurements carried out at 4 K, relatively to the sample grown at 520ºC.